The Canadian Mineralogist
Vol. 36, pp. 1017-1027 (1998)

TRICLINIC MUSCOVITE: X-RAY DIFFRACTION, NEUTRON DIFFRACTION AND PHOTO-ACOUSTIC FTIR SPECTROSCOPY

JIAN-JIE LIANG AND FRANK C. HAWTHORNE[1]

Department of Geological Sciences, University of Manitoba Winnipeg, Manitoba R3T 2N2

IAN P. SWAINSON

Atomic Energy of Canada Limited, Chalk River Laboratories, Chalk River, Ontario K0J 1J0

ABSTRACT

Details of the H site in muscovite were determined using single-crystal neutron-diffraction data collected at room temperature and powder neutron-diffraction data collected at 12 K. Single-crystal neutron-diffraction data, collected at room temperature by Rothbauer (1971), were re-examined using a split-site model for H in the space group *C*2/*c*. Low-temperature neutron-diffraction data were used to evaluate the thermal-vibrational effect on the distribution of nuclear density at the H sites. The separation of the two sites is wider (0.78 Å) at 12 K, but separate nuclear-density maxima were not observed. At least two unique OH stretching bands are revealed by FTIR PAS (Fourier-Transform InfraRed PhotoAcoustic Spectroscopy) experiments. The intensity ratio of the component bands changes as the mirror speed varies, allowing detection of individual stretching bands in severely overlapped spectra. This result confirms that there are two distinct OH groups in the structure of the muscovite examined here. Collectively, these results indicate that there are two distinct H-atom positions in the structure of this muscovite, either disordered with long-range *C*2/*c* symmetry or ordered with lower symmetry. Long-exposure precession photos recorded at room temperature show weak *h*0*l* (*l* odd) reflections that violate *c*-glide symmetry, assumed to exist in muscovite designated as the polytype $2M_1$. Single-crystal peak-profiling also revealed similar well-defined reflections that are confirmed to be Bragg reflections, and not due to double diffraction. Combined with previous second-harmonic generation data on muscovite, these results indicate $C\bar{1}$ symmetry for this sample of muscovite. The driving force for the symmetry lowering from *C*2/*c* to $C\bar{1}$ in muscovite involves cooperative ordering of H atoms over two distinct positions in the structure.

Keywords: muscovite, triclinic symmetry, H-atom positions, neutron diffraction, Rietveld structure refinement, Fourier-transform infrared photo-acoustic spectroscopy.

SOMMAIRE

Nous avons étudié les détails du site occupé par l'hydrogène dans la muscovite au moyen de diffraction de neutrons sur cristal unique à température ambiante et sur poudre à 12 K. Les données prélevées par Rothbauer (1971) sur cristal unique à température ambiante ont été ré-examinées pour évaluer un modèle à sites H partagés dans le groupe spatial *C*2/*c*. Les données de basse température ont été utilisées pour évaluer les effets de vibration thermique sur la distribution de densité des noyaux sur les sites H. La séparation des deux sites est plus importante (0.78 Å) à 12 K, mais nous n'avons pas vu de maxima distincts dans la distribution des noyaux. Au moins deux bandes uniques d'étirement OH sont évidentes dans les spectres obtenus par spectroscopie infra-rouge photo-acoustique avec transformation de Fourier. Le rapport des intensités de ces bandes change selon la vitesse du miroir, ce qui permet la détection des bandes individuelles d'étirement dans ces spectres superposés. Ce résultat confirme la présence de deux groupes OH distincts dans la structure de la muscovite, au moins dans l'échantillon choisi. Pris dans l'ensemble, ces résultats montrent qu'il y a deux positions atomiques distinctes occupées par l'hydrogène dans cette structure. L'occupation de ces positions est soit désordonnée sur une grande échelle selon la symétrie *C*2/*c*, soit ordonnée, avec comme conséquence une symétrie moins élevée. Des clichés de précession à température ambiante montrent des réflexions faibles de type *h*0*l* (*l* impair) en violation du plan de glissement *c*, supposé exister dans la muscovite identifiée comme polytype $2M_1$. Le profil de réflexions individuelles générées par cristaux uniques révèle aussi une bonne résolution de pics distincts obéissant à la loi de Bragg, et non attribuable au phénomène de diffraction double. Ces observations, considérées avec les données antérieures portant sur les deuxièmes harmoniques de la muscovite, indique la symétrie $C\bar{1}$ pour cet échantillon. La réduction de la symétrie *de C*2/*c* à $C\bar{1}$ dans la muscovite implique la mise en ordre complémentaire des atomes H sur deux positions distinctes dans la structure.

(Traduit par la Rédaction)

Mots-clés: muscovite, symétrie triclinique, position des atomes H, diffraction de neutrons, affinement de Rietveld, spectroscopie infra-rouge photo-acoustique avec transformation de Fourier.

[1] *E-mail address:* frank_hawthorne@umanitoba.ca

Introduction

Locating H atoms in minerals has always been difficult, as H is a very weak scatterer of X-rays. It is usually omitted from structure models in X-ray studies of muscovite (Güven 1971, Richardson & Richardson 1982, Liang & Hawthorne 1996), although Schultz *et al.* (1989) did include the H atom in their model of the muscovite structure. Single-crystal neutron diffraction (Rothbauer 1971) gave accurate information about the position of H in muscovite, but with a very large anisotropic displacement of the H atom [amplitude up to 14 times greater than those of other atoms in the structure, although the powder neutron-diffraction study of Catti *et al.* (1994) does not show such large anisotropy of the H atom]. Schultz *et al.* (1989) reported on a sample of muscovite with triclinic symmetry, which would require two distinct H-atom positions. Despite extensive spectroscopic work (Serratosa & Bradley 1958, Bassett 1960, Vedder & McDonald 1963, Wada & Kamitakahara 1991), the question of OH orientation and the number of unique OH groups in muscovite remain unclear.

TABLE 1. UNIT FORMULAE (apfu) OF THE MUSCOVITE CRYSTALS WHICH ARE DISCUSSED HERE

	*LH	*SST	*R
Si	3.068	2.979	3.037
$^{[4]}$Al	0.932	1.021	0.963
ΣT	4.000	4.000	4.000
$^{[6]}$Al	1.954	1.929	1.884
Fe	0.029	0.002	0.143
Mn	0.013	0.006	0.005
Mg	–	0.003	0.014
Li	–	0.035	–
ΣM	1.996	1.975	2.046
K	0.876	0.892	0.889
Na	0.096	0.077	0.092
Rb	0.010	0.021	–
Ca	–	0.001	–
	0.982	0.991	0.981
F	0.256	0.164	0.196
OH	(1.744)	2.016	(1.804)
	2.000	2.180	2.000

References: LH: Liang & Hawthorne (1996); SST: Schultz *et al.* (1989); R: Rothbauer (1971)

Experimental

The muscovite sample used here is from the Himalaya mine, Mesa Grande, California. Liang & Hawthorne (1996) reported the chemical composition and both single-crystal and Rietveld refinements of the structure. Table 1 lists the unit formula of this and other muscovite samples discussed in the text.

Precession photography

A single-crystal precession camera was used to obtain zero-level precession photographs using Zr-filtered Mo$K\alpha$ X-radiation. Exposures of up to one week were taken to test for possible deviations from *C*2/*c* symmetry, focusing particularly on *h*0*l* reflections. Diffraction patterns at precession angles of 25 and 30° were obtained to identify double-diffraction effects, as a specific double diffraction cannot occur at two different precession angles.

Peak profiling of weak h0l (l odd) reflections using a single-crystal diffractometer

The same muscovite crystal used in the precession work was mounted on an automated single-crystal four-circle diffractometer. Peak profiles of the very weak *h*0*l* (*l* odd) reflections were obtained by step-scanning the corresponding peaks over a 2θ-range of up to 2° using 100 to 120 steps with a counting time of 5 minutes per step. For one of such reflection, $20\bar{1}$, scans in different orientations, corresponding to different psi-angles (rotation about the diffraction vector), were taken to ensure that the reflection observed is not due to double diffraction (a double diffraction can only be observed at one specific psi-angle, whereas a Bragg diffraction is observed throughout the complete range of psi angles).

Powder neutron diffraction at 12 K

Powder neutron-diffraction data for muscovite were collected at 12 K in a liquid-He cryostat using the sample of Liang & Hawthorne (1996) loaded into a vanadium can. The intensity data were collected over a 48-hour period on the high-resolution powder diffractometer at the C2 beam-hole of the NRU reactor at the Chalk River Laboratories, Ontario. A wavelength of 1.5022(1) Å, calibrated with Al_2O_3 powder, was used in the data collection. The detector collects data simultaneously over an 80° range of scattering angles with an angular separation of the wires of 0.1°. The scattering range of 8 to 118° was covered by setting the detector in low- and high-angle positions in sequence. A second set of data was collected with the detector at positions of 0.05° offset to those of the first set, giving intensity data at a step interval of 0.05° 2θ.

Fourier-Transform Infrared Photo-Acoustic Spectroscopy (FTIR PAS)

Fourier-Transform Infrared Photo-Acoustic Spectroscopy (FTIR PAS) differs from conventional FTIR spectroscopy in that the IR band-intensity distribution is not only a function of absorbance of the sample and IR frequency (as in transmission IR spectroscopy), but is also strongly dependent on the thermal-diffusion

length, μ, of the sample (Spencer 1986, Choquet *et al.* 1986), which is defined as

$$\mu = \sqrt{(2k/\rho C \omega)} \quad (1)$$

where k, ρ, C are the thermal conductivity, density and specific heat of the sample, respectively, and ω is the modulation frequency of the light, given by

$$\omega = 2\pi V \nu \quad (2)$$

for a Michelson interferometer in which ν is the IR frequency and V is the mirror velocity of the interferometer. The IR intensity is given (Teng & Royce 1982) by

$$q = B \cdot \frac{(\beta\mu)}{\sqrt{(\beta\mu)^2 + 2(\beta\mu) + 2}} \quad (3)$$

where B is a constant independent of the optical-absorption coefficient, β. From the partial derivative of the intensity, q, with respect to the mirror speed, V,

$$\frac{\partial q}{\partial V} = \frac{\partial q}{\partial \mu} \cdot \frac{\partial \mu}{\partial V} = \frac{B\beta\,[(\beta\mu) + 2]}{[(\beta\mu)^2 + 2(\beta\mu) + 2]^{\frac{3}{2}}} \cdot \left(-\frac{1}{2}\mu \cdot \frac{1}{V}\right) \quad (4)$$

it can be seen that the IR intensity will vary with the mirror speed in a complex way that involves (among other factors) the mirror speed, V, and the thermal-diffusion length, μ. The thermal-diffusion length is dependent on ν_1 the IR frequency, (equations 1 and 2), and hence the rate of change of the intensity (the absolute value of ∂q/∂V) is frequency-dependent also. Therefore, the intensity ratio of two adjacent IR bands will change in response to varying mirror speed. This is the property of FTIR PAS that is used here to show that there is more than one OH-stretching band in the IR spectrum of muscovite.

The spectra were recorded with a Bio–Rad FTS–60A (Bio–Rad, Cambridge, Massachusetts) spectrometer fitted with a MTEC Model 200 photo-acoustic cell (MTEC, Ames, Iowa) and accompanying preamplifier and power supply. The sample tray was filled with uncompacted powdered sample. The photo-acoustic cell and the sample were then purged with dry helium. A high-surface-area carbon-black sample (MTEC) was used as the reference material for all spectra. Different interferometer mirror-speeds, corresponding to average modulation frequencies of 5, 10, 50, 100, 400 and 2500 Hz, respectively, were used in the collection of the spectra. The number of scans varied, depending on the mirror speed (modulation frequency) used. The resolution of the spectra is 4 cm^{-1}. Other experimental details can be found in Sowa & Mantsch (1994).

Structure Refinement

Single-crystal neutron diffraction at room temperature

The program SHELXTL PC™ was used for the structure refinement. The coherent neutron-scattering lengths (in femtometers) are $b_O = 5.803$, $b_H = -3.7409$, $b_{Si} = 4.1491$, $b_{Al} = 3.449$, $b_K = 3.71$ (Koester 1977). The single-crystal neutron-diffraction data of Rothbauer (1971) were used for refinement of the H position in the structure; all 625 reflections in the original study were included. The space group, the unit-cell dimensions and the non-H atom positional parameters of Rothbauer (1971) were used as input parameters. However, two H-atoms (each with 0.5 site occupancy) were inserted in the starting model. During initial refinement of the structure, only the positional, displacement and site-occupancy parameters of the two H atoms were varied. The isotropic-displacement factors of the two H-sites were refined independently, and the site occupancies were refined without constraint. The complete structure, including position and anisotropic-displacement parameters for all atoms, was varied to convergence in the final cycles of refinement.

Rietveld refinement at 12 K

The structure of muscovite at 12 K was refined using the program LHPM3 [originally written as DBW3.2 by Wiles & Young (1981) and modified by Hill & Howard (1986)]. Details of the procedure can be found in Liang & Hawthorne (1996). Parameters pertinent to the refinement are listed in Table 2.

Precession Photography and Extinction Conditions

Long-exposure zero-level precession photographs were taken at two different values of the precession angle, as this procedure distinguishes between diffraction maxima that violate the reflection conditions for the presence of non-lattice translational-symmetry elements, and diffractions that are due to double diffraction.

All elements of translational symmetry give rise to what are often colloquially known as "systematic

TABLE 2. POWDER-DIFFRACTION INTENSITY-DATA COLLECTION AND DETAILS OF RIETVELD REFINEMENT OF MUSCOVITE AT 12 K

a	5.1628(7)	Space group	*C2/c*
	5.1765(4)*		
	5.1918(2)**	2θ scan-angle (°)	16–117
		step interval (°2θ)	0.05
b	8.962(1)	max. intensity (counts)	7234
	8.9872(6)*		
	9.0153(5)**	Unique reflections	779
		Structural parameters	46
c	19.977(3)	Experimental parameters	9
	20.072(1)*	N–P	1968
	20.0457(7)**	R_P	1.8
		R_{WP}	2.4
β (°)	95.738(12)	R_{EXP}	1.6
	95.756(6)*	R_{BRG}	0.46
	95.735(3)**		

* room-temperature (Liang & Hawthorne 1996)
** room-temperature (Rothbauer 1971)

absences" in the diffraction pattern; in practice, the presence of such elements of symmetry imposes restrictions on the indices of the reflections that can be observed, and "violations" of such restrictions indicate that the corresponding symmetry element is not present. Thus for the space group $C2/c$ of muscovite-$2M_1$, the presence of the C-centered lattice imposes the index restriction $h + k = 2n$ for all hkl reflections, and the c-glide orthogonal to b imposes the index restriction $l = 2n$ for reflections of the form $h0l$; these conditions are rigorous for normal (Bragg) diffraction. There are two effects that can confuse this situation: (1) double diffraction, and (2) mis-setting of the pulse-height analyzer in the detection system.

Double diffraction: As its name implies, this occurs when a diffracted X-ray beam meets the criterion for diffraction from a second "plane", whereupon it is diffracted again. When such double-diffracted radiation encounters the detection system (counter or film), it overlaps with a normal Bragg diffraction. In most cases, the intensities of these double-diffracted reflections contribute only slightly to a few Bragg reflections. However, where a Bragg reflection is "systematically absent" owing to the presence of an element of translational symmetry, the (weak) double diffraction can be observed, "violating" the index restriction of the symmetry element and apparently indicating that the symmetry element is not present. Double diffraction can affect the index restrictions associated with screw axes and glide planes, such as the c-glide in the $C2/c$ muscovite-$2M_1$ structure. Double diffraction does not affect the index restrictions associated with a non-primitive space lattice, as the selection of a non-primitive space lattice is purely a decision of the crystallographer; the same lattice can be described by a (lower symmetry) primitive space-lattice. One can differentiate between a Bragg diffraction-maximum and a maximum due to double diffraction by varying the instrumental settings such that the Bragg condition is satisfied for a variety of settings; in this case, the Bragg diffraction is always observed. This procedure corresponds to rotating the crystal about the scattering vector (often denoted as psi); for a precession camera, it involves taking photographs at two (or more) values of the precession angle (and other camera settings), whereas for a four-circle diffractometer, it involves recording the Bragg intensities of the same reflection at a variety of settings of the psi angle. A double diffraction has two diffraction conditions to satisfy, and changing the instrumental settings by rotating the crystal about the scattering vector must break the condition for double diffraction. Hence recording a diffraction pattern under two (or more) different instrumental conditions allows differentiation between true "violating" Bragg reflections and reflections due to double diffraction.

Pulse-height analyzer setting: If the pulse-height analyzer in the detection system is wrongly set, harmonics of the diffracted radiation may enter the counting system of the diffractometer. This can give rise to apparent Bragg reflections that "violate" the restrictions for the presence of translational symmetry (as well as augment the intensities of true general Bragg reflections). This is another possible source of error in evaluating the symmetry of a crystal, and should be checked out when making these measurements.

Results

Precession photographs and profiles of weak h0l (l odd) reflections

Precession photos with $\mu = 25$ and 30° are shown in Figure 1. The corresponding indexing is given in Figure 2. Profiles of a selected number of $h0l$ (l odd) reflections are shown in Figure 3. Profiles for one such reflection, $20\bar{1}$, at different psi-angles are given in Figure 4.

Single-crystal neutron-diffraction study at room temperature

The H positions determined by structure refinement using the neutron-diffraction data of Rothbauer (1971) at room temperature are shown in Table 3, and the final positional parameters of the muscovite structure are given in Table 4. Structure refinement using a single H-atom model gave an R-index of 3.9% and a weighted R-index of 4.3%; refinement using a split H-atom model gave an R-index of 3.9% and a weighted R index of 4.2%, respectively. The non-H atom part of the structure is not significantly affected by the different models for the H-atom site (Table 4). There is approximately a 50:50 occupancy of the split-site H-atom positions.

Powder neutron-diffraction study at 12 K

The unit-cell dimensions of muscovite at 12 K are compared with those at room temperature in Table 2; final atomic coordinates and cation occupancies are given in Table 4. Selected interatomic distances and angles of muscovite at different temperatures are given in Table 5. The observed and calculated diffraction-patterns are shown in Figure 5. A comparison of the nuclear-density distribution for the H sites at room temperature and at 12 K is given in Figure 6. There is a

TABLE 3. H POSITIONS IN MUSCOVITE *C2/c* DETERMINED FROM SINGLE-CRYSTAL NEUTRON-DIFFRACTION DATA AT ROOM TEMPERATURE WITH THE NON-HYDROGEN ATOMS FIXED

	H(1)		H(2)
x	0.3652(19)	*x*	0.3883(24)
y	0.6560(12)	*y*	0.6384(16)
z	0.0521(10)	*z*	0.0720(14)
O–H(1) (Å)	0.967(12)	O–H(2) (Å)	0.899(20)

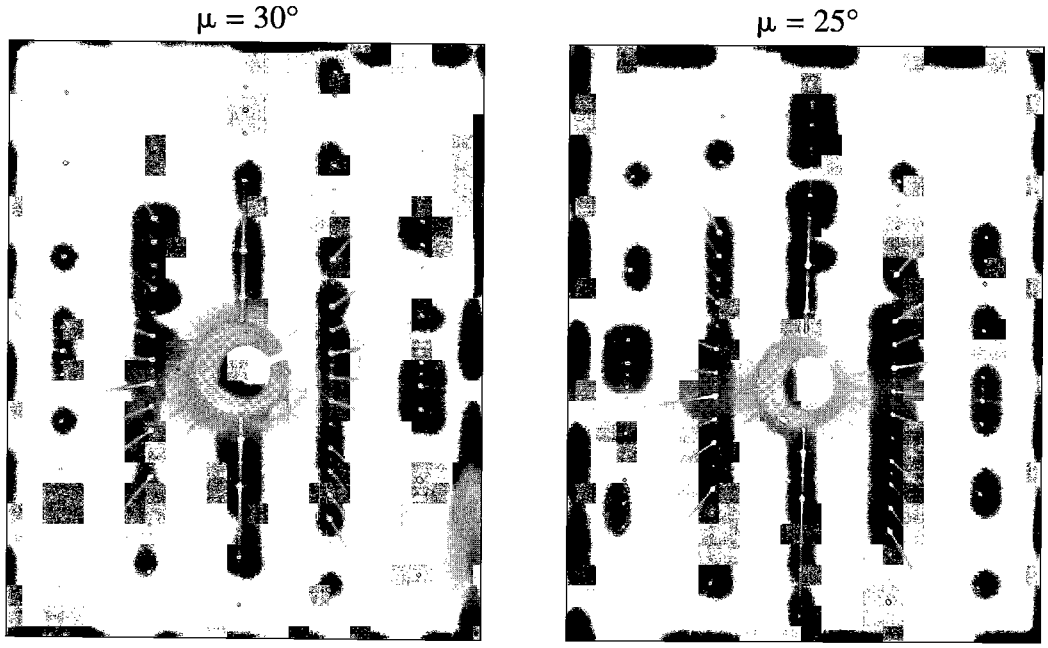

FIG. 1. Zero-level precession photographs of muscovite-2M_1 at μ = 25 and 30°, respectively.

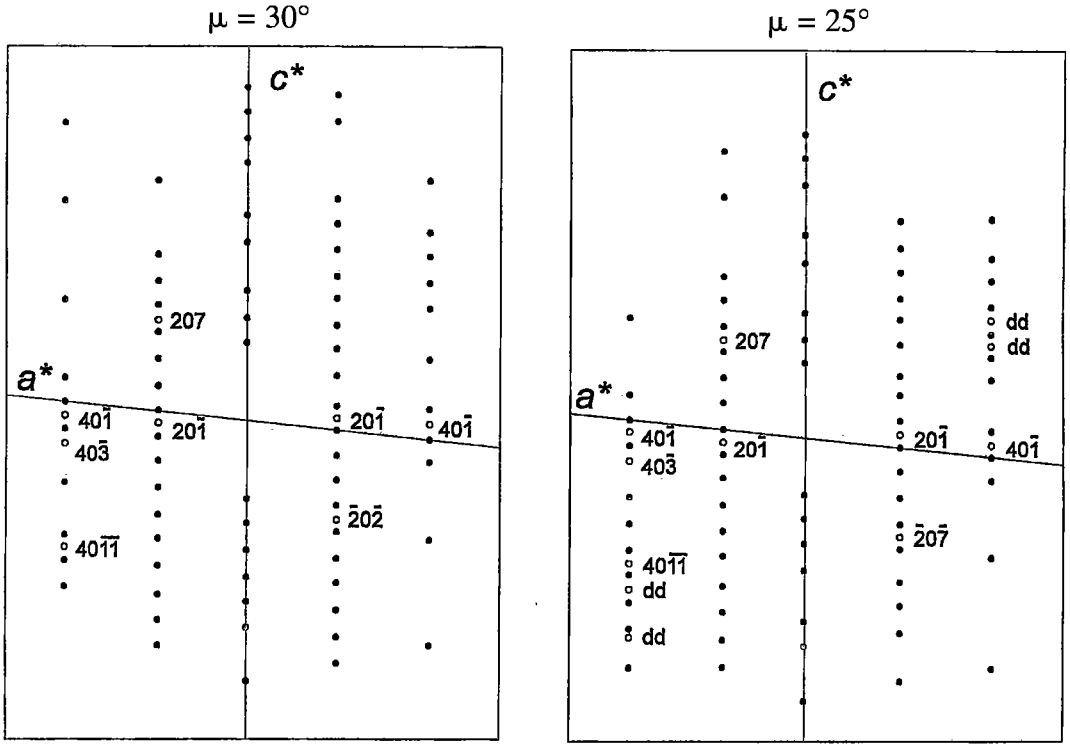

FIG. 2. Partial indexing of the precession photos of muscovite in Figure 1. Solid circles represent reflections conforming to symmetry $C2/c$. Open circles represent reflections violating c-glide symmetry. Note the existence of double diffractions (labeled "dd").

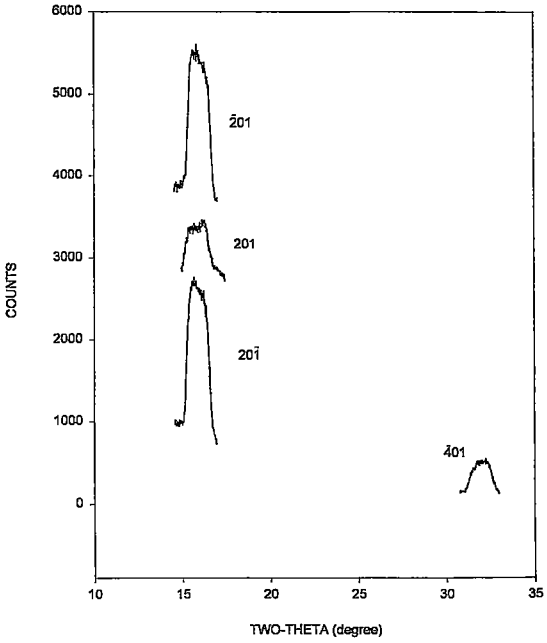

FIG. 3. Peak profiles of selected $h0l$ (l odd) reflections in muscovite-2M_1. Intensities of $20\bar{1}$ and $\bar{2}01$ were raised by 2600 and 3600 counts, respectively, for clarity.

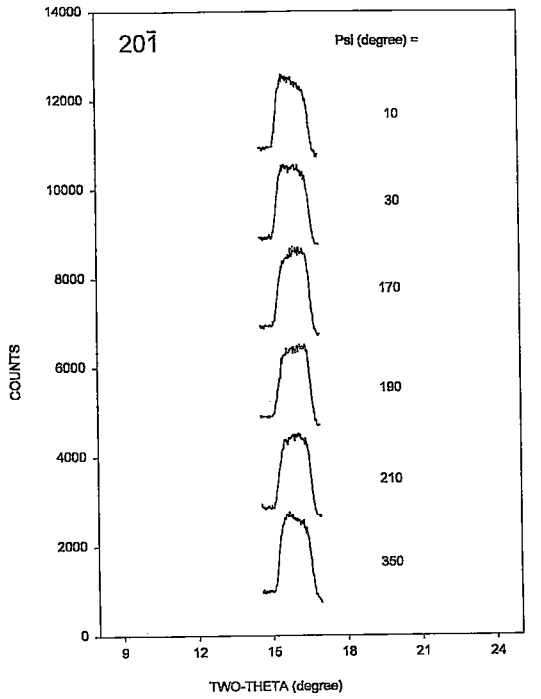

FIG. 4. Peak profiles of the reflection $20\bar{1}$ of muscovite at different psi-angles. The intensities of all profiles, except at psi = 350%, were increased appropriately for clarity.

TABLE 4. ATOMIC COORDINATES OF THE FINAL REFINED STRUCTURE OF MUSCOVITE IN SPACE-GROUP SYMMETRY *C2/c*

	x	*y*	*z*	occupancy
		*Room temperature		
Al	0.2501(6)	0.0838(3)	0.0001(1)	1.10(2)
T(1)	0.4650(5)	0.9291(2)	0.1356(1)	0.96(2)
T(2)	0.4514(5)	0.2581(3)	0.1356(1)	0.99(2)
O(1)	0.4172(4)	0.0929(2)	0.1682(1)	1
O(2)	0.2505(4)	0.8106(2)	0.1577(1)	1
O(3)	0.2504(4)	0.3702(2)	0.1686(1)	1
O(4)	0.4609(4)	0.9428(2)	0.0534(1)	1
O(5)	0.3859(3)	0.2514(2)	0.0534(1)	1
OH	0.4566(4)	0.5628(2)	0.0502(1)	1
K	0	0.0978(5)	1/4	0.50(1)
H(1)	0.3656(19)	0.6560(13)	0.0522(10)	0.50(6)
H(2)	0.3883(25)	0.6380(17)	0.0720(15)	0.36(6)
		12 K		
Al	0.264(6)	0.082(2)	0.001(2)	0.94(3)
T(1)	0.464(4)	0.930(2)	0.137(1)	0.92(4)
T(2)	0.449(4)	0.261(3)	0.134(1)	0.99(5)
O(1)	0.408(8)	0.091(12)	0.167(1)	1
O(2)	0.253(10)	0.801(8)	0.157(1)	1
O(3)	0.247(3)	0.368(2)	0.167(1)	1
O(4)	0.457(3)	0.949(2)	0.052(1)	1
O(5)	0.382(4)	0.253(2)	0.054(1)	1
OH	0.460(5)	0.560(2)	0.050(1)	1
K	0	0.092(4)	1/4	0.48(2)
H(1)	0.392(4)	0.668(2)	0.052(5)	0.49(6)
H(2)	0.402(3)	0.632(2)	0.088(3)	0.41(5)
		Rothbauer (1971)		
Al	0.2502(4)	0.0835(2)	0.00008(8)	1.11(1)
T(1)	0.4646(3)	0.9291(2)	0.13553(8)	0.96(1)
T(2)	0.4516(3)	0.2581(2)	0.13559(8)	0.97(1)
O(1)	0.4167(3)	0.0927(1)	0.16829(6)	1
O(2)	0.2505(3)	0.8107(1)	0.15783(7)	1
O(3)	0.2502(3)	0.3703(1)	0.16869(6)	1
O(4)	0.4610(2)	0.9432(1)	0.05343(6)	1
O(5)	0.3859(2)	0.2515(1)	0.05348(5)	1
OH	0.4566(3)	0.5627(2)	0.05018(6)	1
K	0	0.0980(3)	1/4	0.50(1)
H	0.3727(7)	0.6499(4)	0.0599(2)	0.88(1)

* re-refinement of the data of Rothbauer (1971)

contraction of cell dimensions upon cooling (Table 2); the contraction in the c dimension (0.1 Å) is an order of magnitude larger than that in the a (0.01 Å) or b (0.02 Å) dimensions, a feature characteristic of phyllosilicates (Bish & Johnston 1993, Bish 1993, Bish & Von Dreele 1989).

FTIR PAS spectra

The FTIR PAS spectra of muscovite between 500 and 4000 cm^{-1} are shown in Figure 7. The interferometer-mirror speed (in modulation frequency) used in collecting the spectrum was 2.5 kHz. Spectra in the OH-stretching region (3200–3900 cm^{-1}) were recorded at a range of mirror speeds from 5 Hz to 2.5 kHz, and are shown in Figure 8.

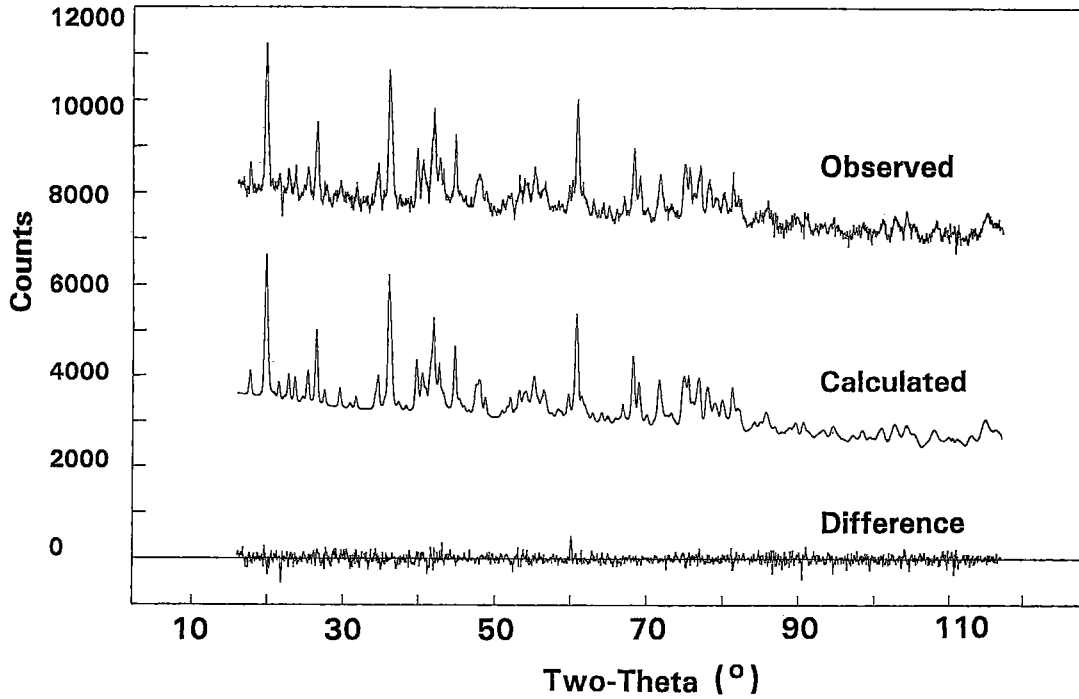

FIG. 5. Observed and calculated neutron-diffraction patterns of muscovite at 12 K. The observed diffraction-pattern has been increased by 5000 counts to avoid pattern overlap.

DISCUSSION

Violation of the space group C2/c

In the zero-level precession photographs (Figs. 1, 2), there are weak (h 0 l) (l odd) reflections violating the c-glide restriction. Peak-profiles (Figs. 3, 4) of these violating reflections are slightly asymmetrical but still well-defined. These violating reflections are present at two distinct values of precession angle, indicating that they are *not* due to double diffraction; they are true Bragg reflections. The presence of these reflections indicates that the space-group symmetry of muscovite is $C2$, $C\bar{1}$ or $C1$ rather than $C2/c$. Similar violating reflections were observed by Schultz *et al.* (1989) on Weissenberg photographs of rose muscovite. However, they did not mention whether or not they had checked for double-diffraction effects, which can commonly result in reflections violating criteria for the presence of non-lattice translational-symmetry elements. This being the case, these reflections are not definitive evidence for the absence of a c-glide plane. Bish *et al.* (1979) and Guggenheim *et al.* (1983) have examined nominally $2M_1$ muscovite samples with the second-harmonic generation method. Their results show no evidence for the absence of a center of symmetry in the muscovite samples they examined. This tends to eliminate both $C2$ and $C1$ as possible space-groups for the muscovite examined here, leaving $C\bar{1}$ as the most likely space-group.

TABLE 5. SELECTED INTERATOMIC DISTANCES (Å) AND ANGLES (°) OF MUSCOVITE (*C2/c*) AT ROOM TEMPERATURE AND 12 K

	room temperature	12 K
<*T*(1)–O>	1.644(1)	1.65(3)
<O–*T*(1)–O>	109.4(8)	109.5(13)
<*T*(2)–O>	1.643(1)	1.63(4)
<O–*T*(2)–O>	109.4(8)	109.4(10)
<Al–O>	1.930(1)	1.92(1)
<K_{inner}–O>	2.859(1)	2.83(3)
<K_{outer}–O>	3.363(2)	3.39(2)
H(1)–O	0.967(12)	1.04(10)
H(2)–O	0.899(20)	1.06(7)
H(1)–H(2)	0.44(3)	0.78(12)
H(1)–O–[001]	95.2(3)	90.5(57)
H(2)–O–[001]	121.7(2)	131.9(27)

H positions at room temperature

Infrared spectra (Serratosa & Bradley 1958, Bassett 1960, Vedder & McDonald 1963, Rouxhet 1970) also provide evidence for more than one OH-orientation in the muscovite structure. The half-width (full-width at

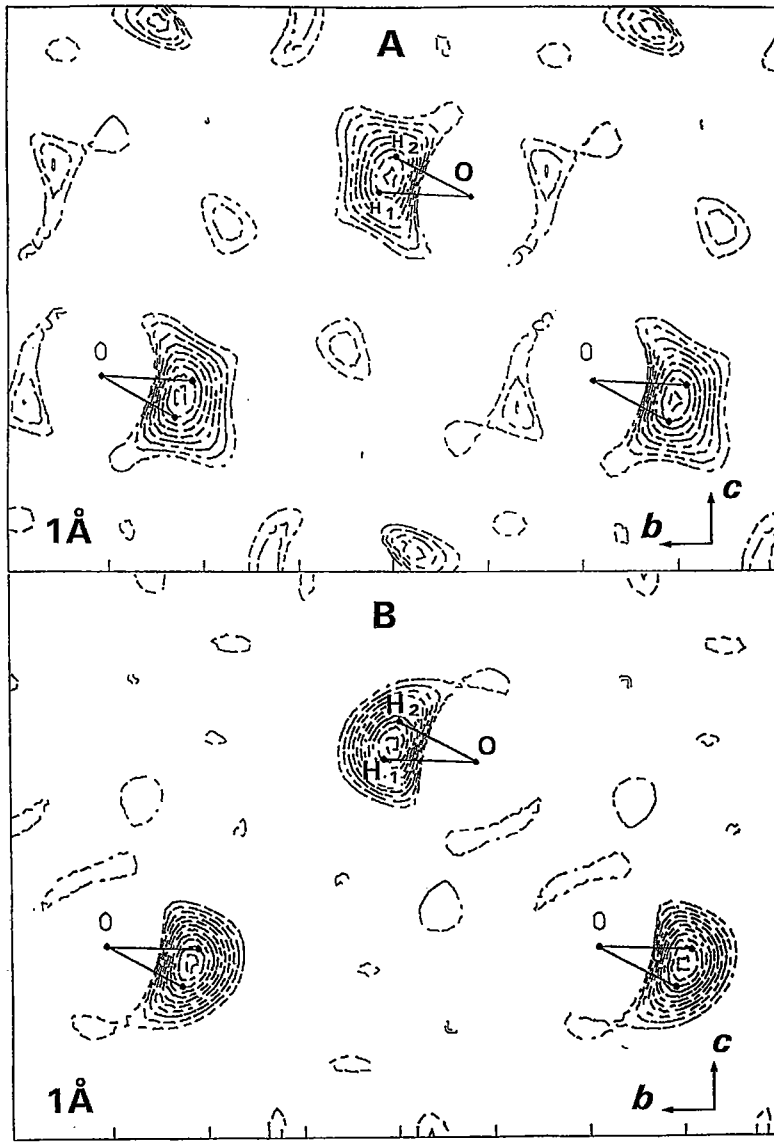

FIG. 6. Difference-Fourier maps projected down [100], showing the nuclear-density distribution in muscovite at (A): room temperature (contours from –10.0 to –2.0) and (B): 12 K (contours from –11.0 to –1.0). The contour interval is 0.1 arbitrary units.

half-height) of the O–H stretching band in muscovite is almost twice as large as in phlogopite (Rouxhet 1970, Bassett 1960, Serratosa & Bradley 1958), irrespective of sample temperature (from 273 to 77 K). The band is also asymmetrical, with the slope toward higher frequency being more gradual than the slope toward lower frequency (Vedder & McDonald 1963). Two OH orientations were suggested by Serratosa & Bradley (1958), in analogy to the OH orientations in lepidolite. Infrared spectroscopy of muscovite at liquid-He temperature may result in increased spectral resolution and provide more conclusive spectral information on this issue.

H position at 12 K

At 12 K, an elongate nuclear-density distribution for the H atom was obtained (Fig. 6B), similar to that observed at room temperature. The muscovite sample used in the present study has a chemical composition

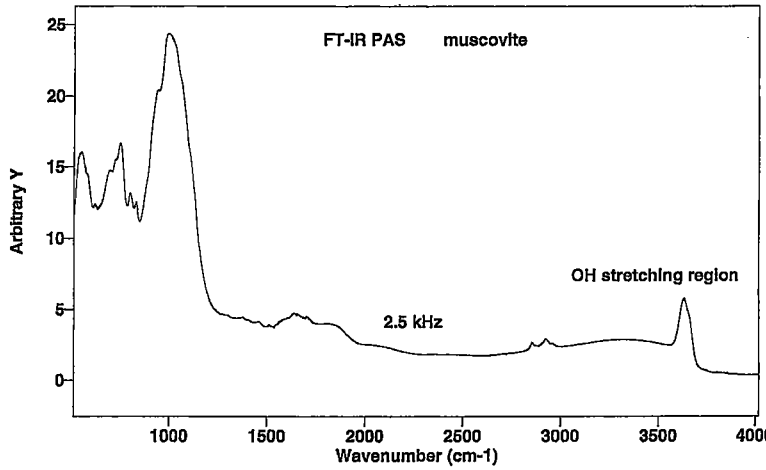

FIG. 7. FTIR PAS of muscovite-2M_1 at room temperature.

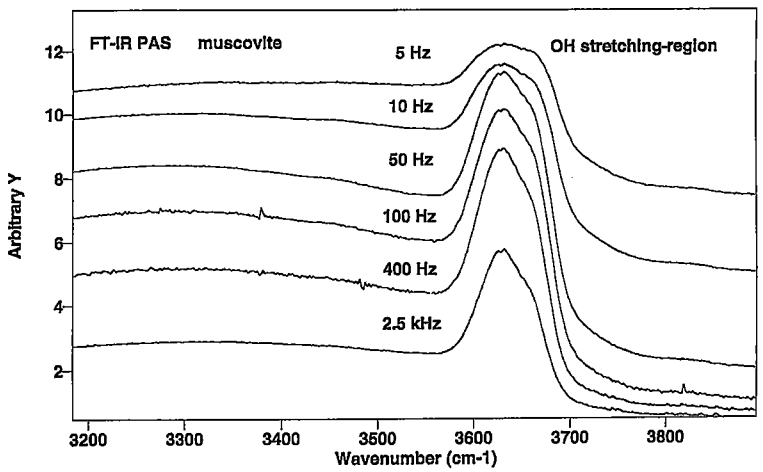

FIG. 8. FTIR PAS spectra of muscovite-2M_1 in the OH-stretching region at room temperature.

similar to that of the sample used by Rothbauer (1971), although the unit-cell parameters of the two samples do differ somewhat (Table 2). The individual O–H distances at 12 K are not significantly different from those at room temperature; however, the H(1)–H(2) separation is significantly larger at low temperature (0.78 Å) than at room temperature (0.44 Å). Such an increase in separation at low temperature supports a split H-atom model. Nevertheless, even with a 0.78 Å separation, it was still not possible to resolve two maxima (Fig. 6B).

Infrared spectroscopy

The FTIR PAS spectrum of muscovite at 2.5 kHz (Fig. 7) shows a shoulder to the high-frequency side of the absorption envelope, and it is separated from the principal maximum by an inflection point; this feature indicates the presence of (at least) two distinct bands in the spectrum. This conclusion is re-inforced by the series of spectra recorded with gradually decreasing interferometer-mirror speed (Fig. 8). The intensity of the high-frequency shoulder increases relative to the maximum intensity of the envelope as the mirror speed decreases from 2.5 kHz to 5 Hz. Note that wavenumber increases toward the right-hand side in Figure 8, and that slower mirror-speed favors higher IR frequencies. The increase in relative intensity of the right shoulder of the envelope indicates that there are two (or more) unique bands in the muscovite spectrum, in turn indicating more than one symmetrically distinct OH group.

Cooperative effects in the muscovite structure

What drives the need for subgroup symmetry in muscovite? Schulz *et al.* (1989) suggested that the lower symmetry is due to the presence of cations at the $M(1)$ site of one layer and not at the $M(1')$ site of the other layer. As the total amount of scattering at the $M(1)$ site in their refinement is low (0.7 *e* $Å^{-3}$), it is difficult to see how such a low occupancy (0.035 Li atoms per formula unit, *apfu*, equivalent to 0.4 electrons per formula unit) at one site could drive a lowering of the symmetry of the crystal, as symmetry-breaking mechanisms require cooperative behavior throughout the whole crystal.

Energy calculations (Abbott *et al.* 1989) and the results of neutron crystal-structure refinement indicate that there are two independent H-atom positions in muscovite. However, these results do *not* indicate whether such positions are long-range ordered or disordered within the structure. The presence of *c*-glide-violating reflections suggests that these H-atom positions *are* actually long-range ordered in the structure. Thus, it seems reasonable to propose that the symmetry-breaking mechanism involves this ordering of the H atoms. Unlike the $M(1)$–$M(1')$ ordering-mechanism proposed by Schulz *et al.* (1989), the atoms involved in a H-bonding mechanism are distributed uniformly throughout the complete crystal, and hence can affect the macroscopic properties of the crystal through local cooperative interactions.

What can cause cooperative ordering of H atoms into two symmetrically distinct positions? Inspection of the structure of muscovite suggests that it must involve short-range order of Al and Si over the T sites in the structure. In this regard, the results of Abbott *et al.* (1989) suggest that the H-atom ordering couples to the local Al–Si arrangement. In this regard, Schulz *et al.* (1989) found a disordered distribution of Al–Si over the tetrahedra in their $C\bar{1}$ refinement of muscovite using X-ray data. Thus, although it now seems established that muscovite can have $C\bar{1}$ symmetry, and that the driving force for the reduction in symmetry involves cooperative ordering of H over two distinct positions in the muscovite structure, the cause of this ordered arrangement of H is still obscure.

Acknowledgements

We thank Steve Guggenheim, Don Peacor, R.J. Swope, anonymous reviewers and the unanonymous editor Bob Martin for their comments on this manuscript. Dr. Petr Černý, University of Manitoba, kindly supplied the muscovite sample. AECL Chalk River Laboratories is acknowledged for the low-temperature neutron-diffraction beam time. Michael Sowa, Institute for Biodiagnostics, National Research Council of Canada (IBD, NRC) helped collect the PAS spectra and offered valuable advice on experimental design and interpretation of the data. IBD NRC allowed us access to the FTIR PAS instrument. This work was supported by the Natural Sciences and Engineering Research Council of Canada in the form of a Graduate Scholarship to J-JL and in the form of Operating, Major Equipment and Infrastructure grants to FCH.

References

Abbott, R.N. Jr., Post, J.E. & Burnham, C.W. (1989): Treatment of hydroxyl in structure-energy calculations. *Am. Mineral.* **74**, 141-150.

Bassett, W.A. (1960): Role of hydroxyl orientation in mica alteration. *Geol. Soc. Am., Bull.* **71**, 449-456.

Bish, D.L. (1993): Rietveld refinement of the kaolinite structure at 1.5 K. *Clays Clay Minerals* **41**, 738-744.

_____, Horsey, R.S. & Newnham, R.E. (1979): Acentricity in the micas: an optical second harmonic study. *Am. Mineral.* **64**, 1052-1055.

_____ & Johnston, C.T. (1993): Rietveld refinement and Fourier-transform infrared spectroscopic study of the dickite structure at low temperature. *Clays Clay Minerals* **41**, 297-304.

_____ & von Dreele, R.B. (1989): Rietveld refinement of the non-hydrogen atomic positions in kaolinite. *Clays Clay Minerals* **37**, 289-296.

Catti, M., Ferraris, G., Hull, S. & Pavese, A. (1994): Powder neutron diffraction study of $2M_1$ muscovite at room pressure and at 2 GPa. *Eur. J. Mineral.* **6**, 171-178.

Choquet, M., Rousset, G. & Bertrand, L. (1986): Fourier-transform photoacoustic spectroscopy: a more complete method for quantitative analysis. *Can. J. Phys.* **64**, 1081-1085.

Guggenheim, S., Schulze, W.A., Harris, G.A. & Lin, Jiuhn-Chorng (1983): Noncentric layer silicates: an optical second harmonic generation, chemical, and X-ray study. *Clays Clay Minerals* **31**, 251-260.

Güven, N. (1971): The crystal structure of $2M_1$ phengite and $2M_1$ muscovite. *Z. Kristallogr.* **134**, 196-212.

Hill, R.J & Howard, C.J. (1986): A computer program for Rietveld analysis of fixed-length X-ray and neutron diffraction patterns. *Australian Atomic Energy Commission, Lucas Heights Research Laboratories (Menai, New South Wales, Australia), Rep.* **M112.**

Koester, L. (1977): Neutron scattering lengths and fundamental neutron interactions. *In* Springer Tracts in Modern Physics – Neutron Physics (W.S. Hohler, ed.). Springer, Heidelberg, Germany (1-55).

Liang, Jian-Jie & Hawthorne, F.C. (1996): Rietveld refinement of micaceous materials: muscovite-$2M_1$, a comparison with single-crystal structure refinement. *Can. Mineral.* **34**, 115-122.

RICHARDSON, S.M. & RICHARDSON, J.W., JR. (1982): Crystal structure of a pink muscovite from Archer's Post, Kenya: implications for reverse pleochroism in dioctahedral micas. *Am. Mineral.* **67**, 69-75.

ROTHBAUER, R. (1971): Untersuchung eines $2M_1$-Muskovits mit Neutronenstrahlen. *Neues. Jahrb. Mineral., Monatsh.*, 143-155.

ROUXHET, P.G. (1970): Hydroxyl stretching bands in micas: a quantitative interpretation. *Clay Mineral.* **8**, 375-388.

SCHULTZ, P.K., SLADE, P.G. & TIEKINK, E.R.T. (1989): Refinement of a muscovite structure in *C* symmetry. *Neues Jahrb. Mineral., Monatsh.*, 121-129.

SERRATOSA, J.M. & BRADLEY, W.F. (1958): Determination of the orientation of OH bond axis in layer silicates by infrared absorption. *J. Phys. Chem.* **62**, 1164-1167.

SOWA, M.G. & MANTSCH, H.H. (1994): FTIR step-scan photoacoustic phase analysis and depth profiling of calcified tissue. *Appl. Spectros.* **48**, 316-319.

SPENCER, N.D. (1986): Listening in on solid materials. *CHEMTECH* (June), 378-384.

TENG, Y.C. & ROYCE, S.H. (1982): Quantitative Fourier transform IR photoacoustic spectroscopy of condensed phases. *Appl. Optics* **21**, 77-80.

VEDDER, W. & MCDONALD, R.S. (1963): Vibrations of the OH ions in muscovite. *J. Chem. Phys.* **38**, 1583-1590.

WADA, N. & KAMITAKAHARA, W.A. (1991): Inelastic neutron- and Raman-scattering studies of muscovite and vermiculite layered silicates. *Phys. Rev.* **B43**, 2391-2397.

WILES, D.B. & YOUNG, R.A. (1981): A new computer program for Rietveld analysis of X-ray powder diffraction patterns. *J. Appl. Crystallogr.* **14**, 149-151.

Received June 1, 1996, revised manuscript accepted June 11, 1998.